Comparison of Ce^{3+}/Yb^{3+} with Er^{3+}/Yb^{3+} down-conversion pairs in YAG host for improving the efficiency of the crystalline silicon solar cells

Xuezhuan Yi (易学专), Hui Lin (林 辉), Chong Chen (陈 冲), and Shengming Zhou (周圣明)*

Shanghai Institute of Optics and Fine Mechanics, Chinese Academy of Sciences, Shanghai 201800, China

**Corresponding author: yixuezhuan881130@126.com*

Received August 02, 2013; accepted October 11, 2013; posted online March 20, 2014

Re^{3+}, Yb^{3+} co-doped $(Re_{0.005}Yb_xY_{(0.995-x)})_3Al_5O_{12}$ [Re = Ce, Er, x = 0, 0.02, 0.05, 0.1, and 0.2] transparent ceramics are synthesized by the solid state reaction and vacuum sintering as the down-conversion (DC) materials. The photoluminescence excitation and the photoluminescence spectra demonstrate the near-infrared quantum cutting (QC) and the energy transfer (ET) from Re^{3+} to Yb^{3+} in both of these series of samples. The comparison of the near-infrared QC spectra of the two series of samples shows that the Ce^{3+}, Yb^{3+} co-doped $Y_3Al_5O_{12}$ transparent ceramic samples have much higher intensity of the emission spectra in the near-infrared region, and higher ET efficiency than the Er^{3+}, Yb^{3+} co-doped ones. So, the Ce^{3+}, Yb^{3+} DC ion pair is a better choice to improve the efficiency of the crystalline silicon-based solar cells.

OCIS codes: 160.5690, 160.4670.

doi: 10.3788/COL201412.S11603.

Crystalline silicon-based solar cells have a history of nearly 60 years[1–3], but the improvement of the efficiency is still a difficult problem. One of the major reasons is the energy loss of the thermalization, which is caused by spectra mismatch. The energy gap of the crystalline silicon (EG_{Si}) is only 1.1 eV, while the strongest emission of the solar spectra is about 350–550 nm ($h\nu$ = 3.5 – 2.3 eV), and this part of energy is roughly twice as high as EG_{Si}. If UV-blue photons are converted into the near-infrared ones efficiently, the energy loss of thermalization may be reduced greatly. So, the quantum cutting (QC) down-conversion (DC) is regarded as a good method to improve the efficiency of the solar cells[4–8]. As the energy of the emission spectra of the Yb^{3+} ion is just above the EG_{Si}, many studies have focused on the Yb^{3+} and Ln^{3+} (Ln = Pr, Tb, Er, Eu, Bi, Ce, etc.) co-doped QC materials[9–14].

The DC involves different types of conversion: cooperative DC, cross-relaxation DC, step photon emission, etc. Ce^{3+}, Yb^{3+} co-doped material is a typical example of cooperate DC[15,16]. One Ce^{3+} ion absorbs one higher-energy photon and transforms the energy to two Yb^{3+} ions at one time, then the excited Yb^{3+} ions emit the near-infrared photons. The Er^{3+}, Yb^{3+} co-doped material is one of the typical cross-relaxation DC[17]. Differences from the cooperative DC system are the excited Er^{3+} ion relaxes to a middle-energy level and transforms the part of energy to one Yb^{3+} ion, then the Er^{3+} ion and the Yb^{3+} ion emit one near-infrared region photon, respectively. Two kinds of ion pairs have their own characteristics, and both can realize the process of DC. In order to know which is more preferable to improve the efficiency of the silicon-based solar cells, a series of YAG transparent ceramic samples co-doped with Ce^{3+}–Yb^{3+} ions and Er^{3+}–Yb^{3+} ions are synthesized, and optical properties and the spectra are also investigated in this work.

Initially, composition of high-purity Al_2O_3 (99.999%), Y_2O_3 (99.999%), Yb_2O_3 (99.999%) and CeO_2 (99.99%) commercial powders are weighed according to the designed $(Ce_{0.005}Yb_xY_{(0.995-x)})_3Al_5O_{12}$ (x = 0, 0.02, 0.05, 0.1, 0.2; named as S0, S1, S2, S3 and S4, respectively). Then, the raw materials added with 0.5 wt% ethyl orthosilicate are mixed by ball milling in ethanol for 24 h, and dried at 80 °C for 48 h. Then, the powder mixtures were first uniaxially pressed into plates at 10 MPa and cold isostatically pressed at 200 MPa. These green bodies are sintered at 1700 °C under a base pressure of approximately 1.0×10^{-3} Pa for 18 h. At last, all the obtained sintered samples are annealed at 1500 °C for 10 h in the air to reduce the oxygen vacancies introduced during the vacuum sintering and the residual stresses. The $(Er_{0.005}Yb_xY_{(0.995-x)})_3Al_5O_{12}$ [x = 0, 0.02, 0.05, 0.1, and 0.2; named as Y0, Y1, Y2, Y3, and Y4, respectively] transparent ceramic samples are also synthesized in the same way as Ce^{3+}, Yb^{3+}: YAG, and the only difference is that the CeO_2 (99.99%) is replaced by the Er_2O_3 (99.999%) as the raw material.

All the specimens were double-side polished to 1.0-mm thick. The photoluminescence excitation (PLE) and the photoluminescence (PL) spectra of the two series of samples are measured by an FLS920 fluorescence spectrometer (Edinburgh Instruments, Britain).

Figure 1 shows the PL and Fig. 2 shows the PLE spectra of S0–S4. The PL spectra are obtained under the excitation at 467 nm, which is the strongest emission in the solar spectra. The emission spectra in the visible region are a broad band with the peak located at about 530 nm due to the 5d→4f transition of Ce^{3+},

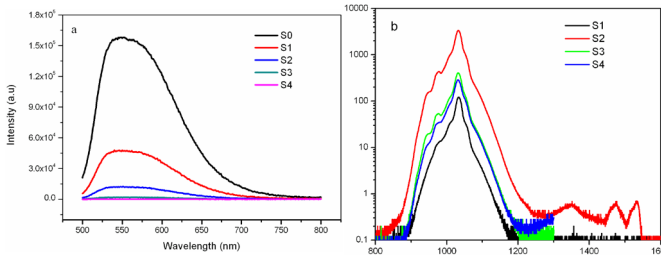

Fig. 1. PL spectra of the samples S0–S4 in the visible (a) and near-infrared region (b).

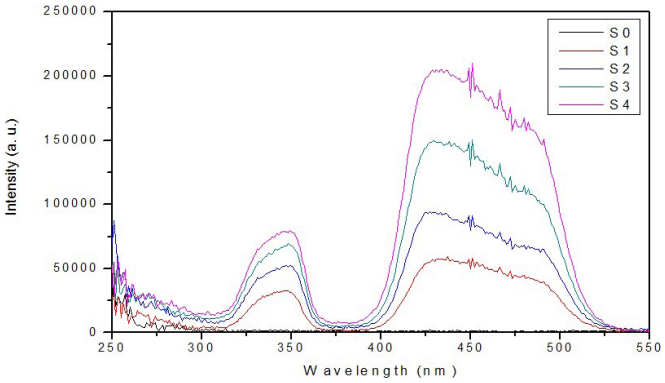

Fig. 2. PLE spectra of the samples S0–S4.

while in the near-infrared region, the emission peaks are located at 1028 and 968 nm corresponding to the Yb^{3+}: $^2F_{5/2}\rightarrow{}^2F_{7/2}$ transition. The intensity of the emission band in the visible region reduces with increase in Yb^{3+} doping concentration. Meantime, however, the intensity of the NIR emission increases and reaches the highest for S2. The variation rule of the PL spectra demonstrated the energy transfer (ET) process from Ce^{3+} to Yb^{3+}. The intensity of the emission peaks for S3 and S4 becoming quite weak indicates the appearance of concentration quenching of Yb^{3+} ions. The ET process could also be verified by the PLE spectra as showed in Fig. 2. Samples S1–S4 are monitored by 1028 nm in the emission spectrum; two strong excitation bands, centered at about 352 and 467 nm due to the Ce^{3+}: $4f\rightarrow5d_2$ and $5d_1$ transition, are observed, while the sample S0 showed no excitation peaks.

The PL and PLE spectra of samples Y0–Y4 are shown in Figs. 3 and 4, respectively. All the samples were excited at 520 nm, and the obtained PL spectra showed strong emission peaks in visible region at 557, 561, 671 and 677 nm, which are attributed to the transition of Er^{3+}: $^2H_{11/2}$; $^4S_{3/2}\rightarrow{}^4I_{15/2}$ and $^4F_{9/2}\rightarrow{}^4I_{15/2}$, respectively, as shown in Fig. 3(a). Er^{3+} ions in the transparent ceramics matrix exhibited some sharp PL emission lines due to intra-4f shell transitions. However, the emission spectrum in the visible region was a broad band for Ce^{3+}, which was due to $5d\rightarrow4f$ transition. Figure 3(b) showed that emission peaks are located at the near-infrared region. In the near-infrared region, the emission peaks of Y1–Y4 are located at 970, 1028 and 1049 nm due to transition of different Stark levels of Yb^{3+}. While for

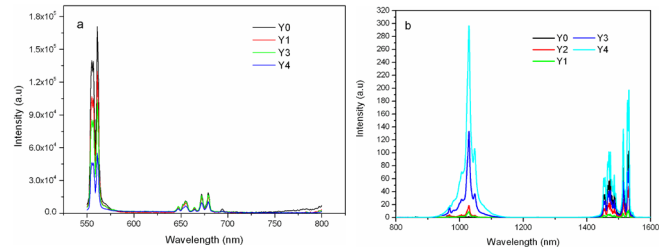

Fig. 3. PL spectra of the samples Y0–Y4 in the (a) visible and (b) near-infrared region.

Y0, the emission peaks are located at 965 and 1008 nm due to the transition of Er^{3+}: $^4I_{11/2}\rightarrow{}^4I_{15/2}$. The emission peaks attributed to the transitions from different Stark energy levels of Er^{3+}: $^4I_{13/2}$ to those of the Er^{3+}: $^4I_{15/2}$ are located at 1471, 1517 and 1531 nm. Figures 3(a) and (b) also showed that with an increase in the doping concentration of Yb^{3+} ions, the intensity of the visible region peaks reduces, while in the near-infrared region, the intensity of the peaks due to the transition of Yb^{3+} ion increases. This proved the ET process from the Er^{3+} ions to the Yb^{3+} ions. However, a part of energy is also transferred to the lower energy levels of the Er^{3+} itself (Er^{3+}: $^4I_{13/2}$), and the intensity of these peaks also increases with an increase in the concentration of Yb^{3+} ions. The ET process during the Er^{3+} itself could be verified by the PLE spectra. When the samples under 1028 and 1500 nm emission are monitored, the excitation peaks due to transition of different energy levels of Er^{3+} ions are found to be located at the same position, as shown in Fig. 4. When compared with the emission spectra of Yb^{3+} ion of sample Y4 in Fig. 3(b) with that of sample S2 in Fig. 1(b), we can observe that the intensity of Y4 was about 2 orders of magnitude smaller than that of S2. This may be due to the lower intensity of the absorption spectra of Er^{3+} ion. Above all, the result showed that the Ce^{3+}, Yb^{3+} ions co-doped YAG transparent ceramic samples had much higher efficiency of conversion of the visible photons to the near-infrared ones.

The schematic energy level diagrams of the Ce^{3+}, Yb^{3+} and Er^{3+} are presented in Fig. 5. It can be clearly observed from Fig. 5 that the energy of the Ce^{3+}: $5d_1\rightarrow4f$ is about twice as high as that of the Yb^{3+}: $^2F_{5/2}\rightarrow{}^2F_{7/2}$, and there were no other energy levels between the two different energy levels, which made

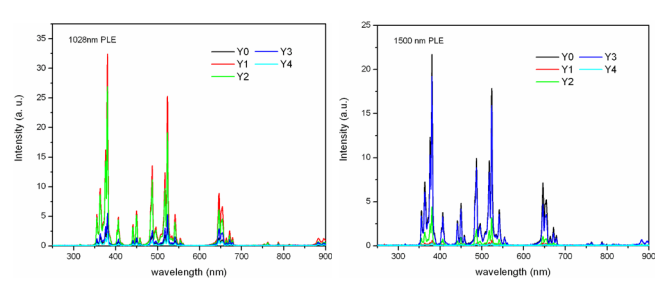

Fig. 4. PLE spectra of the samples Y0–Y4 under 1028 and 1500-nm emission monitored.

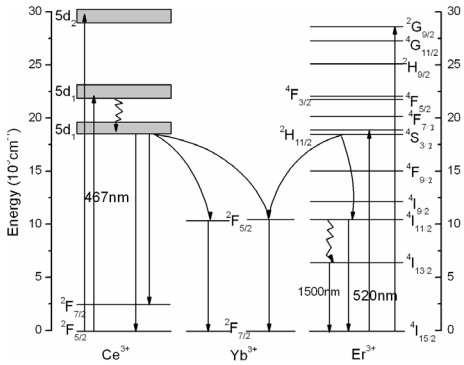

Fig. 5. Schematic energy level diagrams of Ce^{3+}, Yb^{3+}, and Er^{3+} illustrating the QC process in the YAG transparent ceramics.

the cooperative DC possible. Although the Ce^{3+} ion had the tendency to become Ce^{4+} ion while Yb^{3+} ion had the tendency to become Yb^{2+} ion, the Ce^{4+}–Yb^{2+} charge transfer state would influence the ET process. Lin *et al.*[16] have concluded that this problem should not influence the cooperate DC much. The ET process of Er^{3+} ion and Yb^{3+} ion is also shown in Fig. 5. When the materials are under the excitation at 520 nm, the cross-relaxation DC would happen as Er^{3+}:$^4S_{3/2}$, $^2H_{11/2}$ + Yb^{3+}:$^2F_{7/2}$→Er^{3+}:$^4I_{11/2}$ + Yb^{3+}:$^2F_{5/2}$, and then the Er^{3+} ion and the Yb^{3+} ion would emit one near-infrared photon as shown in Fig. 5. However, the electron of Er^{3+}:$^4I_{11/2}$ energy level also easily relaxes to the Er^{3+}:$^4I_{13/2}$ level by a nonradioactive process, and then a relatively smaller near-infrared photon than that of the Yb^{3+} ion is emitted. The intensity of these emission peaks due to the transition between Er^{3+}: $^4I_{13/2}$ and Er^{3+}: $^4I_{15/2}$ is comparative to that of the Yb^{3+} ions, especially when the Yb^{3+} ion is heavily doped, as shown in Fig. 3(b). The results indicated that the Ce^{3+}, Yb^{3+}: YAG transparent ceramic samples are more preferable to use to improve the efficiency of the silicon-based solar cells.

The PL and PLE spectra show that the ET exists in the Ce^{3+}, Yb^{3+} and Er^{3+}, Yb^{3+} co-doped YAG transparent ceramics. At the same time, a part of energy is also transferred to the lower energy levels of Er^{3+} in the Er^{3+}/Yb^{3+} DC pairs. This part of energy is wasted for crystalline Si solar cells. Although the Ce^{3+}, Yb^{3+}: YAG transparent ceramics had the problem of the QC of Yb^{3+} ions, the intensity of the emission peaks in the near-infrared region and the efficiency of the ET process both are higher than that of the Er^{3+}, Yb^{3+} co-doped ones. Hence, the Ce^{3+}, Yb^{3+} DC ion pair is a better and appropriate choice to use to improve the efficiency of the silicon-based solar cells.

This work was supported by the National Natural Science Foundation of China (No. 51172254 and No. 51202269) and the Science and Technology Commission of Shanghai Municipality (No. 10JC1415700).

References

1. B. Oregan and M. Gratzel, Nature **353,** 737 (1991).
2. W. U. Huynh, J. J. Dittmer, and A. P. Alivisatos, Science **295,** 2425 (2002).
3. M. Law, L. E. Greene, J. C. Johnson, R. Saykally, and P. D. Yang, Nat. Mater. **4,** 455 (2005).
4. T. Trupke, M. A. Green, and P. Wurfel, J. Appl. Phys. **92,** 1668 (2002).
5. P. Vergeer, T. J. H. Vlugt, M. H. F. Kox, M. I. den Hertog, J. P. J. M. van der Eerden, and A. Meijerink, Phys. Rev. B **71,** 014119 (2005).
6. Q. Y. Zhang, G. F. Yang, and Z. H. Jiang, Appl. Phys. Lett. **91,** 051903 (2007).
7. D. Timmerman, I. Izeddin, P. Stallinga, I. N. Yassievich, and T. Gregorkiewicz, Nat. Photon. **2,** 105 (2008).
8. K. Deng, T. Gong, L. Hu, X. Wei, Y. Chen, and M. Yin, Opt. Express **19,** 1749 (2011).
9. D. Serrano, A. Braud, J. L. Doualan, P. Camy, A. Benayad, V. Menard, and R. Moncorge, Opt. Mater. **33,** 1028 (2011).
10. Z. Wang, Y. Wang, Y. Li, and H. Zhang, J. Mater. Res. **26,** 693 (2011).
11. J. J. Eilers, D. Biner, J. T. van Wijngaarden, K. Kraemer, H. U. Guedel, and A. Meijerink, Appl. Phys. Lett. **96,** 151106 (2010).
12. Yu, T. Jiajia, Z. Song, and Y. Jianrong, Q. J. Electrochem. Soc. **157,** A1073 (2010).
13. X. T. Wei, J. B. Zhao, Y. H. Chen, M. Yin, and Y. Li, Chinese Phys. B **19,** 077804 (2010).
14. J. Chen, H. Guo, Z. Li, H. Zhang, and Y. Zhuang, Opt. Mater. **32,** 998 (2010).
15. D. Chen, Y. Wang, Y. Yu, P. Huang, and F. Weng, Opt. Lett. **33,** 1884 (2008).
16. H. Lin, S. Zhou, H. Teng, Y. Li, W. Li, X. Hou, and T. Jia, J. Appl. Phys. **107,** 043107 (2010).
17. S. Xiao, X. Yang, and J. W. Ding, Appl. Phys. B Laser. Opt. **99,** 769 (2010).